JOC*Article*

Improved Imide Receptors by Imprinting Using Pyrimidine-Based Fluorescent Reporter Monomers

Panagiotis Manesiotis, Andrew J. Hall,* and Börje Sellergren*

INFU, Universität Dortmund, D-44221 Dortmund, Germany

borje@infu.uni-dortmund.de; andy@infu.uni-dortmund.de

Received December 17, 2004

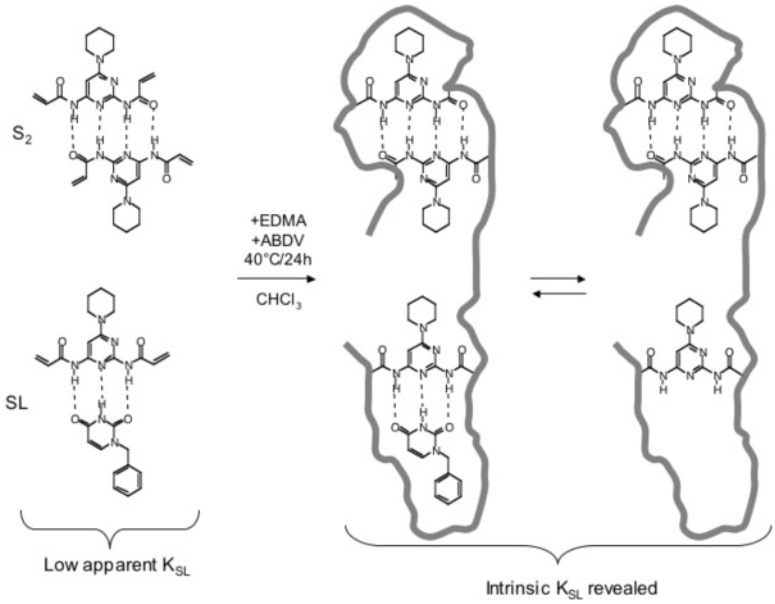

Optically responsive receptors toward imides based on 6-substituted 2,4-bis(acrylamido)pyrimidines are presented. The monomers were readily prepared in good yield. Solution binding to 1-benzyluracil (**BU**) monitored by ^{1}H NMR appeared lower than a previously reported pyridine-based monomer. However, as indicated by ^{1}H NMR and IR spectral investigations, the association strength was demonstrated to be "masked" by dimerization of the pyrimidine-based monomer units. Thus, from dilution experiments, a dimerization constant of 731 M^{-1} was estimated for the pyrimidine-based monomer 2,4-bis(acrylamido)-6-piperidinopyrimidine whereas for the pyridine-based monomer 2,6-bis(acrylamido)pyridine, no self-association was observed. This precluded an accurate determination of the binding constant for **BU** to the former monomer whereas for the latter a binding constant of 757 M^{-1} was measured. Despite the strong self-association, the novel monomer was shown to lead to enhanced imprinting effects when compared to imprinted polymers prepared analogously, but using the pyridine-based monomer as the recognition element. This was attributed to a higher intrinsic binding affinity exhibited by the pyrimidine based host monomer *vis à vis* the guest and the existence in the former of more than one interaction site for the guest. The monomers exhibited fluorescence emission informative of the mode of monomer incorporation in the polymer and the presence of guest species. Thus, the fluorescence was rapidly and selectively quenched upon template addition, with the degree of quenching correlating with binding affinity and the amount of template bound to the polymer.

Introduction

Molecular imprinting of polymer matrixes has become a widely used approach to generate robust macromolecular receptors for one or a group of target molecules.[1−5] Thus, polymerization is performed in the presence of a template molecule and a complementary functional mono-

(1) *Molecularly imprinted polymers. Man made mimics of antibodies and their applications in analytical chemistry*; Sellergren, B., Ed.; Elsevier Science B.V.: Amsterdam, 2001; Vol. 23.

10.1021/jo0477906 CCC: $30.25
Published on Web 03/10/2005

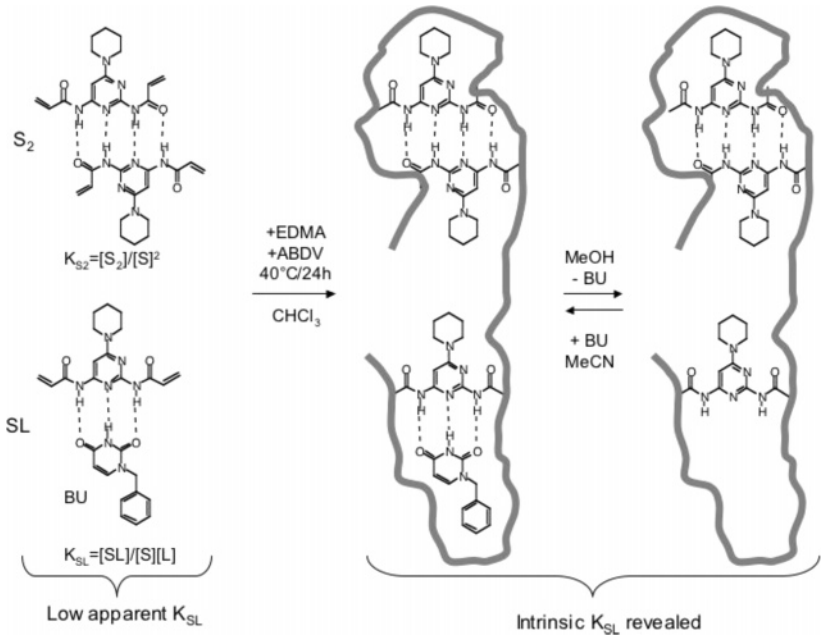

FIGURE 1. Modes of incorporation of monomer **2** in the imprinting of **BU**.

mer, such that binding sites complementary in both shape and functionality to the original template are formed.

Although simple commodity-type monomers have proven successful for the imprinting of a large variety of small target molecules, the binding affinity and capacity are often insufficient for the corresponding application. One such example is the binding of the imide structural motif.[6−9] Whereas the traditional monomers lead to polymers performing poorly, monomers presenting a donor−acceptor-donor hydrogen bonding array, notably 2,6-bis(acrylamido)pyridine **(1)**, have proven to yield highly discriminating sites for the RNA/DNA bases uracil and thymine[7,8] and for cyclobarbital,[9] albeit mostly in noncompetitive solvents.

In our previous work, we used **1** as the functional monomer in the preparation of molecularly imprinted polymers targeted toward 1-benzyluracil (**BU**).[8] The solution association constant for binding between **1** and **BU** was found to be of moderate strength ($K_a = 757\ M^{-1}$ in $CDCl_3$) and the performance of the subsequently prepared MIPs was better than those prepared using other designed monomers, based on aminopurines, which exhibited lower association constants with **BU** in solution. To further enhance the monomer−template association we have embarked on the design of readily synthesized monomers exhibiting enhanced solution binding properties *vis-à-vis* imides. We anticipated that the novel functional monomers **2** and **3** would satisfy these criteria for the following reasons: (1) The introduction of electron-releasing groups at the 6-position of the 2,4-bis(amido) pyrimidine skeleton will increase the basicity of the N3 ring nitrogen, thereby making it a stronger hydrogen-bond acceptor.[10] (2) The choice of lipophilic 6-position substituents leads to an enhancement in solubility of the monomers in comparison to **1.** This will allow higher template loads and correspondingly higher saturation capacities of the resulting polymers to be achieved. (3) The nonequivalence of the hydrogen bond donating amido protons may create a better match toward imides with nonequivalent hydrogen bond accepting carbonyl oxygens.

In this paper, we report on the synthesis, solution-binding properties, and polymerization of these monomers for the imprinting of **BU**. We show that **2** leads to imprinted polymers performing better than **1** for this task and attribute this to a higher intrinsic binding constant which is masked by strong self-association in solution (Figure 1).

In addition, a second interaction mode between **2** and **BU** appears at higher concentrations. Binding of **BU** to imprinted polymers made from either **1** or **2** is accompanied by quenching of the polymer fluorescence, making the new polymers potentially interesting for the design of new receptor layers for chemical sensors.

Experimental Section

3′-Azido-3′-deoxythymidine (AZT) was from Sigma (St. Loius, MO), and 2,2′-azobis(2,4-dimethylvaleronitrile) (ABDV) was purchased from Wako (Japan). These reagents, together with 2,4-diamino-6-chloropyrimidine, 2,6-diaminopyridine, acryloyl chloride, piperidine and sodium, uracil, and thymine were used as received.

(2) *Molecularly Imprinted Materials − Sensors and other Devices*; Shea, K. J., Roberts, M. J., Yan, M., Eds.; Materials Research Society Symposium Proceedings: San Fransisco, 2002; Vol. 723, M1.3.

(3) *Molecular Imprinting − From Fundamentals to Applications*; Komiyama, M., Takeuchi, T., Mukawa, T., Asanuma, H., Eds.; Wiley-VCH: Weinheim, 2002.

(4) Wulff, G. *Chem. Rev.* **2002**, *102*, 1−27.

(5) Haupt, K.; Mosbach, K. *Chem. Rev.* **2000**, *100*, 2495−2504.

(6) Lanza, F.; Hall, A. J.; Sellergren, B.; Bereczki, A.; Horvai, G.; S.; Cormack, P. A. G.; Sherrington, D. C. *Anal. Chim. Acta* **2001**, *435*, 91−106.

(7) Kugimiya, A.; Mukawa, T.; Takeuchi, T. *Analyst* **2001**, *126*, 772−774.

(8) Hall, A. J.; Manesiotis, P.; Mossing, J. T.; Sellergren, B. *Mater. Res. Soc. Symp. Proc.* **2002**, *723*, M1.3.1−5.

(9) Tanabe, K.; Takeuchi, T.; Matsui, J.; Ikebukuro, K.; Yano, K.; Karube, I. *J. Chem. Soc., Chem. Commun.* **1995**, *22*, 2303−2304.

(10) Abraham, M. H.; Duce, P. P.; Prior, D. V.; Barrat, D. G.; Morris, J. J.; Taylor, P. J. *J. Chem. Soc., Perkin Trans. 2* **1989**, 1355−1375.

Ethylene glycol dimethacrylate (EDMA) was purified by the following procedure prior to use: the received material was washed consecutively with 10% aqueous NaOH, water, brine, and finally water. After drying over $MgSO_4$, pure, dry EDMA was obtained by distillation under reduced pressure.

2,6-Bis(acrylamido)pyridine (**1**),[11] 1-benzyluracil **(BU),** and 1,3-dibenzyluracil **(DBU)**[12] were prepared as previously described. Deuterated solvents were purchased from Deuterio GmbH (Kastellaun, Germany). Anhydrous tetrahydrofuran was stored over appropriate molecular sieves. All other solvents were reagent grade or higher.

NMR spectra were recorded at 400 MHz. High-resolution mass spectra were obtained using a JEOL JMS-SX-102A mass spectrometer. All melting points are uncorrected.

Synthesis of 2,4-Bis(acrylamido)-6-piperidinopyrimidine (2). 2,4-Diamino-6-piperidinopyrimidine[13] (20 mmol, 3.87 g) and triethylamine (50 mmol, 5.06 g) were dissolved in THF (50 mL), and the solution was cooled to 0 °C under N_2. To the cooled, stirred solution was added, dropwise, a solution of acryloyl chloride (45 mmol, 4.07 g) in THF (20 mL). After addition, stirring was continued overnight at ambient temperature under N_2. After this time the reaction mixture was partitioned between chloroform (100 mL) and water (40 mL), and the layers were separated. The organic layer was washed, consecutively, with saturated aqueous $NaHCO_3$ (2 × 100 mL) and water (100 mL) before being dried over $MgSO_4$. After filtration and evaporation of solvent, ethanol (100 mL) was added to the obtained solid and the mixture stirred for 2 h. After filtration, the yellow solid was recrystallized from ethanol to give the product as light yellow crystals in 60% yield: mp polymerized before melting at 213 °C; ^{1}H NMR (DMSO-d_6) δ 1.48−1.49 (m, 4H), 1.59−1.60 (m, 2H), 3.536 (t, 4H), 5.67−5.76 (2 × d, 2H), 6.18−6.27 (2 × d, 2H), 6.60−6.70 (2 × dd, 2H), 7.25 (s, 1H), 9.97 (s, 1H), 10.38 (s, 1H); ^{13}C NMR (DMSO-d_6) δ 24.0, 25.0, 44.6, 85.4, 127.2, 128.1, 131.3, 131.9, 156.4, 158.1, 163.1, 163.2, 164.4; HRMS calcd 301.1539, found 301.1501.

Synthesis of 2,4-Bis(acrylamido)-6-ethoxypyrimidine (3). Preparation as for **2**, starting from 2,4-diamino-6-ethoxypyrimidine.[14] Recrystallization from ethanol gave the product as light yellow crystals in 65% yield: mp polymerized before melting at 217 °C; ^{1}H NMR (DMSO-d_6) δ 1.27−1.30 (t, 3H), 4.29−4.34 (q, 2H), 5.73−5.80 (2 x d, 2H), 6.22−6.31 (2 x d, 2H), 6.61−6.72 (2 x dd, 2H), 7.20 (s, 1H), 10.41 (s, 1H), 10.73 (s, 1H); ^{13}C NMR (DMSO-d_6) δ 14.7, 62.7, 90.2, 129.3, 131.3, 156.8, 159.5, 165.0, 171.1; HRMS calcd 262.1066, found 262.1049.

Synthesis of 2-(Acrylamido)-6-(propylamido)pyridine (4). Monoacylation of 2,6-diaminopyridine with propionic acid anhydride was achieved following the method of Berl et al.[15] Column chromatography (acetone/*n*-hexane 4/6) yielded 2-amino-6-(propylamido)pyridine as a white solid in 50% yield: mp 142−143 °C; ^{1}H NMR (DMSO-d_6) δ 0.96−1.00 (t, 3H), 2.25−2.31 (q, 2H), 5.65 (s, 2H), 6.09−6.11 (d, 1H), 7.17−7.19 (d, 1H), 7.25−7.29 (t, 1H), 9.72 (s, 1H); ^{13}C NMR (DMSO-d_6) δ 9.3, 29.0, 100.5, 102.9, 138.5, 150.2, 158.1, 172.1; HRMS calcd 165.0902, found 165.0875. This monoacylated compound was then reacted with one equivalent of acryloyl chloride in the presence of triethylamine. After basic, aqueous workup and evaporation of the dried organic solution, the compound was obtained as a white solid in 40% yield: mp 158−159 °C; ^{1}H NMR (DMSO-d_6) δ 1.01−1.04 (t, 3H), 2.34−2.40 (q, 2H), 5.72−7.75 (d, 1H), 6.23−6.28 (d, 1H), 6.58−6.64 (dd, 1H), 7.70−7.80 (m, 3H), 9.95 (s, 1H), 10.25 (s, 1H); ^{13}C NMR (DMSO-d_6) δ 9.2, 29.1, 108.9, 109.1, 127.4, 131.3, 139.7, 149.9, 150.2, 163.4, 172.6; HRMS calcd 219.1008, found 219.0984.

Synthesis of 2,4-Bis(propylamido)pyridine (5). This compound was prepared from 2,6-diaminopyridine and propionic acid anhydride following the method of Feibush et al.[16] Recrystallization from ethyl acetate gave the product as white crystals in 40% yield: mp 149 °C; ^{1}H NMR (DMSO-d_6) δ 1.00−1.04 (t, 6H), 2.23−2.39 (q, 4H), 7.67−7.70 (m, 3H), 9.923 (s, 2H); ^{13}C NMR (DMSO-d_6) δ 9.8, 29.7, 109.2, 140.2, 150.7, 173.2; HRMS calcd 221.1164, found 221.1188.

Synthesis of 2,4-Bis(propylamido)-6-piperidinopyrimidine (6). The same procedure as described above for **5** was followed: mp 223−224 °C; ^{1}H NMR (DMSO-d_6) δ 0.97−1.00 (2 × t, 6H), 1.47−1.48 (m, 4H), 1.56−1.59 (m, 2H), 2.32−2.38 (q, 2H), 2.46−2.52 (q, 2H), 3.49−3.51 (t, 4H), 7.11 (s, 1H), 9.54 (s, 1H), 10.03 (s, 1H); ^{13}C NMR (DMSO-d_6) δ 8.9, 9.0, 23.9, 24.8, 29.2, 29.3, 44.5, 84.2, 159.3, 158.0, 163.0, 172.6, 173.6; HRMS calcd 305.1852, found 305.1952.

^{1}H NMR Titrations and Estimation of Association Constants. All ^{1}H NMR titrations were performed in $CDCl_3$. Association constants (K_{SL}) for the interactions between hosts and guests were determined by titrating an increasing amount of functional monomer into a constant amount of guest (**BU**). The concentration of **BU** was 1 mM, and the amounts of added monomer (**1**, **2**, or **3**) were 0, 0.5, 1, 2, 3, 4, 5, 7.5, and 10 equiv, respectively. The complexation-induced shift ($\Delta\delta$) of the guest imide proton was followed and titration curves were then constructed of $\Delta\delta$ versus **BU** concentration. The raw titration data were fitted to a 1:1 binding isotherm by nonlinear regression using Microcal Origin 5.0 from which the association constants could be calculated.[17] Dilution experiments were performed with **1** and **2** over the concentration range 0.0836−10 mM; the changes in chemical shifts of the amido protons were followed, and the dimerization constant (K_{S2}) was estimated in a similar manner as above. In an attempt to estimate the binding constant between **BU** and **2**, the free concentration of **2** was calculated by taking dimerization of **2** into account as

$$[S] = -\frac{1}{4K_{S2}} + \sqrt{\frac{1}{16K_{S2}^{\,2}} - \frac{1}{2K_{S2}}\left(\frac{\Delta\delta}{\Delta\delta_{max}}L_t - S_t\right)} \quad (1)$$

where [S] = concentration of free **2**; $\Delta\delta$ = the complexation-induced shift of the imide proton of **BU**; $\Delta\delta_{max}$ = estimated complexation induced shift at saturation; L_t = total concentration of **BU**; and S_t = total concentration of **2**.

FT-IR Characterization. IR spectra were recorded on an FT-IR spectrometer equipped with an ATR accessory. Samples (1 mL) of 5 mM solutions of **1**, **2**, and **BU** in chloroform were evaporated on the surface of an ATR crystal. Spectra (32 scans) were recorded after disappearance of the solvent signals under continuous purging with dry nitrogen.

Polymer Preparation. Imprinted polymers (**P1**, **P2**) were prepared in the following manner. The template molecule **BU** (0.2 mmol), the respective functional monomer (**1** or **2**) (0.3 mmol), and EDMA (20 mmol) were dissolved in chloroform (5.6 mL). To the solution was added the initiator ABDV (1% w/w total monomers). The solution was transferred to a glass tube, cooled to 0 °C, and purged with a flow of dry nitrogen for 10 min. The tubes were then flame-sealed while still under cooling. The tubes were then placed in a thermostated water bath (pre-set at 40 °C), thus initiating the polymerization which was then allowed to continue at this temperature for 24 h. After this time, the tubes were broken and the polymers lightly crushed. Removal of the template molecule from the polymers was achieved by extraction with methanol in a

(11) Oikawa *J. Polym. Sci.: Part A: Polym. Chem.* **1993**, *31*, 457−465.

(12) Kundu, N. G.; Sidkar, S.; Hertzberg, R. P.; Schitz, S. A.; Khatri, S. G. *J. Chem. Soc., Perkin Trans.* **1985**, *1,* 1295−1300.

(13) Roth, B.; Smith, J. M.; Hulquist, J. M. E. *J. Am. Chem. Soc.* **1950**, *72*, 1914−1918.

(14) Roth, B.; Smith, J. M.; Hulquist, J. M. E. *J. Am. Chem. Soc.* **1951**, *73*, 3, 2864−2868.

(15) Berl, V.; Schmutz, M.; Krische, M. J.; Khoury, R. G.; Lehn, J.-M. *Chem. Eur. J.* **2002**, *8*, 1227−1244.

(16) B. Feibush, A. Figueroa, R. Charles, K. D. Onan, P. Feibush, B. L. Karger, *J. Am. Chem. Soc.* **1986**, *108*, 3310−3318.

(17) Connors, K. A. *Binding constants. The measurement of molecular complex stability*; John Wiley & Sons: New York, 1987.

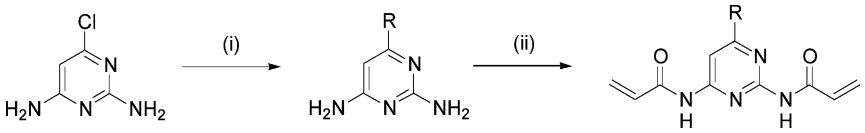

FIGURE 2. Synthesis of monomers **2** and **3**. Conditions: (i) **2**, R = $C_5H_{10}N$: piperidine, reflux; **3,** R = OEt: NaOEt, EtOH, reflux; (ii) acryloyl chloride, Et_3N, 0 °C to rt.

Soxhlet apparatus for 24 h. Thereafter, the polymers were crushed and sieved to obtain a particle size of 25−50μm. Nonimprinted polymers (NIPs) ($\mathbf{P_N1}$, $\mathbf{P_N2}$) were prepared in the same way as described above, but with the omission of template molecule from the pre-polymerization solution.

Anal. Calcd: **P1** C, 60.6; H, 7.1; N, 0.34. Found: C, 61.1; H, 7.2; N, 0.45. $\mathbf{P_N1}$ C, 60.6; H, 7.1; N, 0.34. Found: C, 61.5; H, 7.5; N, 0.5. **P2** C, 60.6; H, 7.1; N, 0.28. Found: C, 59.7; H, 7.6; N, 0.3. $\mathbf{P_N2}$ C, 60.6; H, 7.1; N, 0.28. Found: C, 60.4; H, 7.4; N, 0.3.

HPLC Evaluation of the Polymers. The 25−50 μm particle size fraction was repeatedly sedimented (80/20 methanol /water) to remove fine particles and then slurry-packed into HPLC columns (125 mm × 5 mm, i.d.) using the same solvent mixture as pushing solvent. Subsequent analyses of the polymers were performed using an HP1050 system equipped with a diode array-UV detector and a work-station. The mobile phase was 100% acetonitrile, the flow rate was 1 mL/min, analyte injection volume was 10 μL, and analyte concentrations were 1 mM. Analyte detection was performed at 260 nm.

Batch Rebinding. Imprinted or nonimprinted polymer (10 mg of 25−50 μm particles) was weighed into 2 mL HPLC vials. Solutions of **BU** in acetonitrile (1 mL) made up to the following concentrations were then added: 0, 0.01, 0.05, 0.1, 0.2, 0.5, 0.75, 1 mM. After 24 h incubation, the supernatants (200 μL) were transferred into the wells of a 96-well quartz plate (HELMA) and the free concentration of **BU** calculated from the UV absorbance (λ = 260 nm) measured using a SAFIRE 96-well plate reader (TECAN). A calibration curve was constructed by measuring the absorbance of standard solutions with the same concentrations as the rebinding solutions and the amount of bound **BU** obtained by subtraction.

Fluorescence Measurements. Imprinted or nonimprinted polymer (10 mg of 25−36μm particles) was weighed into the wells of a 96-well quartz plate. Solutions of **BU** in acetonitrile (200 μL) made up to the following concentrations were then added: 0, 0.01, 0.05, 0.1, 0.2, 0.5, 0.75, 1 mM. The fluorescence emission (λ_{ex} = 270 nm, λ_{em} = 340 nm) of the sedimented particles was monitored in the bottom reading mode until no further change in intensity was observed (ca. 30 min).

Results and Discussion

Functional Monomer Synthesis, Solution Conformation, and Binding Studies. The two-step synthesis of the new functional monomers reported herein is illustrated in Figure 2.

Nucleophilic substitution of the 6-chloro group of 2,4-diamino-6-chloropyrimidine is achieved by reaction with piperidine or sodium ethoxide, leading to the intermediate 2,4-diamino-6-substituted pyrimidines. Reaction of these with 2 equiv of acryloyl chloride in the presence of triethylamine yields the novel monomers **2** and **3** as crystalline solids in good yield.

^{1}H NMR titrations were performed with the monomers **2** and **3** using the same procedure previously used for **1**, with **BU** serving as the guest compound. The complexation induced shift of the imide proton of **BU** was followed in both cases and is shown in Figure 3. Based on the previous, extensive documentation of analogous host−guest systems[18−21] we have assumed a 1:1 stoichiometry of the association of both **2** and **3** with **BU**. Disregarding self-association, nonlinear curve fitting of the isotherm[17] gave apparent association constants for both **2** (K_a = 596 ± 85 M^{-1}) and **3** (K_a = 561 ± 37 M^{-1}) that were lower than that obtained for **1** (K_a = 757 ± 28 M^{-1}). We noted, however, that the imide proton of **BU** shifted downfield more than twice when interacting with **1** than with **2** or **3**. Although this could in principle be explained by a different local magnetic environment, the magnitude of the difference suggested other causes. It occurred to us that strong self-association of **2** and **3** would lead to a similar behavior, resulting in a "false" saturation curve. Indeed, compounds such as **2** are known to self-associate via the structure (S_2) shown in Figure 1, where the amide at position 2 adopts an energetically unfavorable *cis*-conformation due to repulsion of the

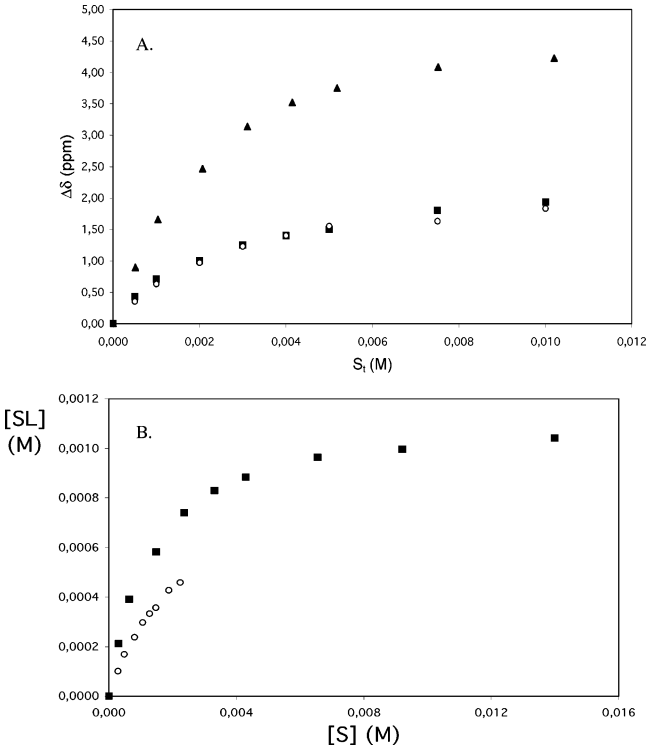

FIGURE 3. (A) ^{1}H NMR complexation induced shifts ($\Delta\delta$) of the **BU** imide proton versus the total concentration of **1** (filled triangles), **2** (filled squares), or **3** (open circles) in $CDCl_3$. (B) Binding isotherms for **1** (filled squares) and **2** (open circles) corresponding to the data in (A) assuming for **1** a 1:1 binding model and for **2** a 1:1 model with dimerization of **2** (K_{S2} = 731M^{-1}, $\Delta\delta_{max}$ = 4.5 ppm).

(18) Sherrington, D. C.; Taskinen, K. A. *Chem. Soc. Rev.* **2001**, *30*, 83−93.
(19) Yu, L.; Schneider, H.-J. *Eur. J. Org. Chem.* **1999**, 1619−1625.
(20) Beijer, F. H.; Kooijman, H.; Speck, A. L.; Sijbesma, R. P.; Meijer, E. W. *Angew. Chem., Int. Ed.* **1998**, *37*, 75−78.
(21) Beijer, F. H.; Sijbesma, R. P.; J. A. Vekemans, J. M.; Meijer, E. W. *J. Org. Chem.* **1996**, *61*, 6371−6380.

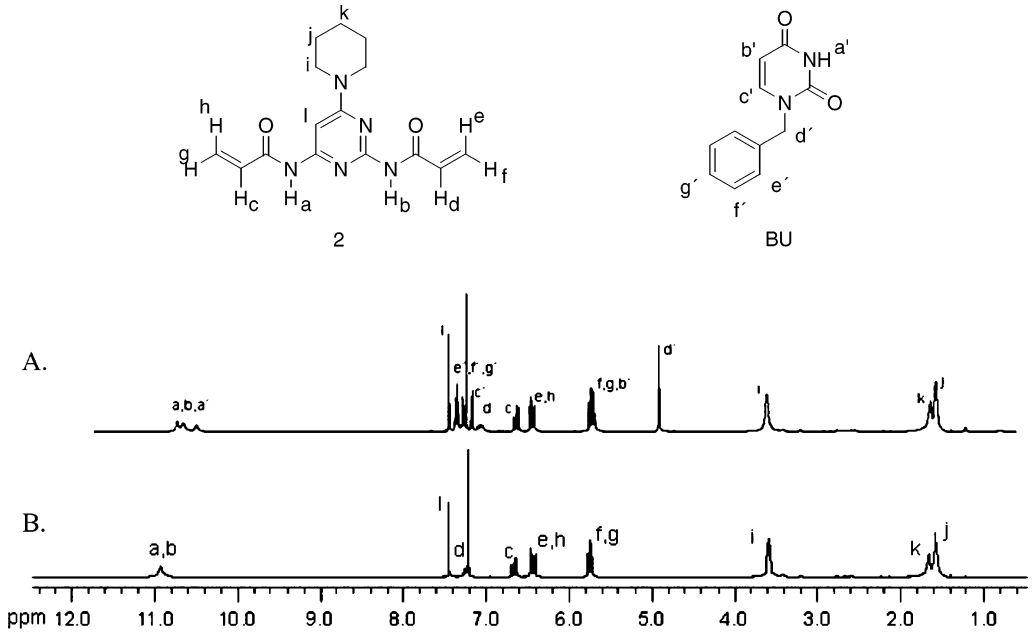

FIGURE 4. ^{1}H NMR spectra of an equimolar mixture of **2** and **BU** (A) and **2** alone (B), present as 5 mM solutions in $CDCl_3$. The shifts are given in Table 2, and the bands correspond to the protons according to the inserted structures.

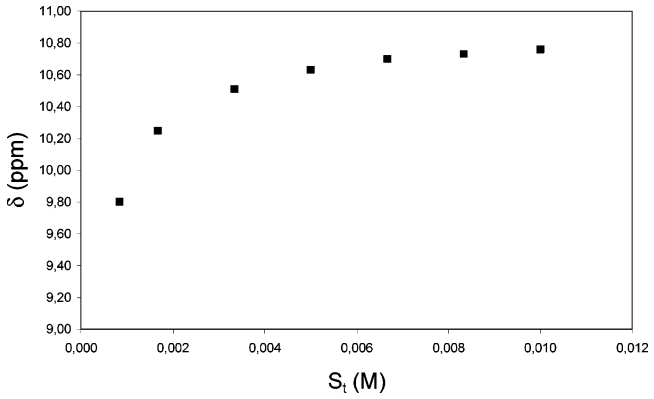

FIGURE 5. ^{1}H NMR dilution experiment showing the shifts (δ) of the amide protons of **2** versus the total concentration of **2** in $CDCl_3$.

carbonyl oxygen by the N1 ring nitrogen.[20] Evidence for this conformation was obtained from the ^{1}H NMR band positions of the vinyl protons c and d of **2** (see Figure 4) which were found as quartets at 6.6−6.7 and 7.2−7.3 ppm in $CDCl_3$ whereas both appeared at 6.6−6.7 ppm in DMSO-d_6. The downfield shift of d is likely due to a weak CH−N hydrogen bond between the N1 ring nitrogen and proton d of the corresponding vinyl group. This would stabilize a *cis*-conformation of the amide group and place the vinyl group nearer to the piperidine ring. In support of this structure, a 2D-NOESY-spectrum of **2** showed positive NOEs between the aliphatic carbons of the piperidine ring (i,j,k) and the corresponding vinyl protons (d,e,f).

The self-association of **1** and **2** was investigated by a ^{1}H NMR dilution experiment. The corresponding spectra revealed significant upfield chemical shift changes of the amide protons of **2** upon dilution (Figure 5), whereas no movements were seen in a similar experiment using **1**.

From the curve in Figure 5 a dimerization constant (K_{S2} as defined in Figure 1) of 731 M^{-1} (±51) was obtained.[17] This value is considerably higher than that previously reported for hexanoic acid (2-hexanoylaminopyrimidine-4-yl)amide (K_{S2} = 170 M^{-1}) by Mejier et al.,[20] but expected since the latter lack the above hydrogen bond stabilization of the amide *cis*-conformation and also the electron-releasing group at the 6-position. Further support for the presence of strong self-association came from IR investigations. In Figure 6 are shown the FT-IR spectra of films of the pure monomers obtained by evaporation of chloroform solutions.

The following peak assignments were made. **1**: 3476, 3402 cm^{-1} CONH free, N−H stretch; 3271 cm^{-1} CONH associated, N−H stretch. **2**: 3316 cm^{-1} trans CONH associated, N−H stretch, 3218 cm^{-1} cis CONH associated, N−H stretch, 2954 cm^{-1} piperidine CH_2, C−H stretch (asym), 2857 cm^{-1} piperidine CH_2, C−H stretch (sym). **BU:** 3166 cm^{-1} imide, N−H stretch; 3042 cm^{-1} phenyl.

The high-frequency region reveals stark differences in the positions of the bands corresponding to the NH stretching mode of the amide groups.[22] Whereas **1** exhibits bands at 3402 and 3476 cm^{-1}, corresponding to nonassociated NHs, **2** exhibits somewhat more intense bands, all below 3316 cm^{-1}, indicative of strong hydrogen bonds. Although we were not able to unambiguously assign the bands in the low-frequency region, we noted that **2** showed bands at frequencies expected for *cis*-amides, whereas no such bands were found in the spectra of **1**. Furthermore, the bands of **2** were generally sharper than those of **1**. This indicates the presence of a defined structure showing little conformational ambiguity.

We thereafter attempted to derive an association constant between **BU** and **2** taking the strong dimerization into account. Assuming a $\Delta\delta_{max}$ of the imide proton of **BU** equal to that obtained in the titration with **1**, it is seen in Figure 3B that the corresponding isotherm only covers the low concentration interval showing no sign of

(22) Colthup, N. B.; Daly, L. H.; Wiberly, S. E. *Introduction to IR and Raman Spectroscopy*, 3rd ed.; Academic Press: New York, 1990.

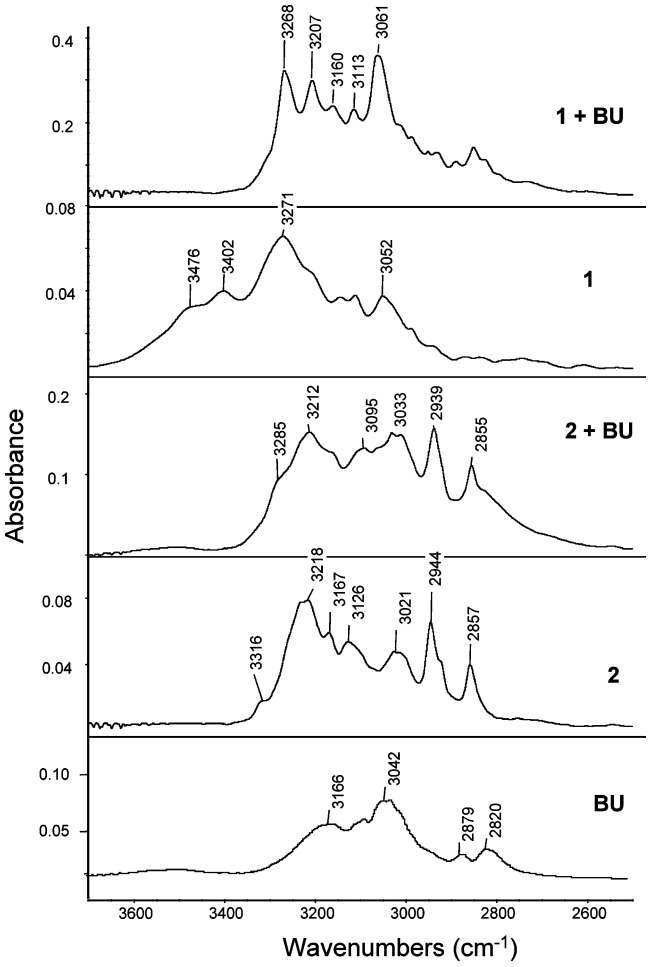

FIGURE 6. ATR FT-IR spectra of films of **1**, **2**, and **BU** and corresponding equimolar mixtures of **1**+**BU** and **2**+**BU** in the high-frequency region, obtained by evaporation of corresponding chloroform solutions on the surface of an ATR crystal.

saturation. Thus, the intrinsic association constant between **BU** and **2** cannot be determined by this method.

Binding Properties of Imprinted Polymers. We thereafter prepared imprinted (MIP) and nonimprinted (NIP) polymers as shown in Figure 1 and packed them into HPLC columns for chromatographic assessment of their ability to retain the template molecule and other analytes of related structure and functionality. This latter group comprises molecules where there exist either additional sites for interaction with the pendant functionalities within the polymer matrixes (uracil (**U**) and 5-fluorouracil (**FU**)), a molecule where a hydrogen-bonding site has been blocked (1,3-dibenzyl uracil (**DBU**)) and a molecule containing a different substituent at the 1-position (**AZT**). The results of the chromatographic evaluation are shown in Table 1.

Opposite to the expectations we had based on the solution-binding results, the polymers prepared using **2** (**P2**) exhibited stronger retention and higher imprinting factors (IF = k_{MIP}/k_{NIP}) than those prepared using **1** (**P1**). As seen in Table 1, the template molecule was nearly two times more retained on **P2** than on **P1**. On injection of the other, similar analytes onto the polymers, the difference between the MIP and NIP becomes even more stark. While the retention of these analytes on the NIP

TABLE 1. Retention Factors (k) and Imprinting Factors (IF) for Uracil- and Thymine-Based Solutes Retained on Polymers P1 and P2[a]

	P1			P2		
solute	k_{MIP}	k_{NIP}	IF	k_{MIP}	k_{NIP}	IF
BU	23	0.93	25	41	1.37	30
U	3.82	0.69	5.5	7.00	1.13	6.1
FU	1.04	0.34	3.1	1.95	0.66	2.9
DBU	0.31	0.28	1.1	0.37	0.35	1.0
AZT	3.46	0.66	5.3	6.62	1.23	5.4

[a] $k = (t_R - t_0)/t_0$, where t_R is the retention time of the analyte and t_0 is the retention time of the nonretained void marker (acetone). IF = k_{MIP}/k_{NIP}. The mobile phase was 100% ACN, the injection volume was 10 μL, analyte concentration was 1 mM, flow rate was 1 mL/min, and detection was performed at 260 nm.

are little different from that of the template molecule, the imprinted polymer shows a high degree of selectivity for its template.

The HPLC retention data, although demonstrating a clear improvement using **2**, are not sufficient for determining its origin. Since only one point on the isotherm is tested, the higher k and IF obtained on **P2** may be due to a larger number of accessible sites, a higher intrinsic binding affinity of these sites or a combination of these effects. To discriminate between these possibilities, complete equilibrium binding isotherms were measured (Figure 7A,B). Small samples (10 mg) of the polymers were incubated with solutions (1 mL) of the template (**BU**) in acetonitrile at different concentrations and the amount of free and bound solute estimated from the supernatant concentrations of **BU** after overnight incubation.

When considered individually, the isotherms described close to straight lines and none of the polymers exhibited visible saturation within the measured concentration interval. This shows that the nonspecific adsorption was weak in acetonitrile although, as indicated by the slope of these curves, a significant number of such weak sites was present. When comparing the isotherms of the imprinted with the nonimprinted polymers, the former were steeper showing that the MIPs had adsorbed more **BU** at a given concentration of free **BU**. This difference was larger for **P2** than for **P1**, which appears more clearly from a plot of the differential adsorptions (Figure 7C). From this we conclude that **P2** contains additional binding sites, which appear to be stronger and to exist in a greater abundance than those of **P1**. These results were supported by fluorescence emission measurements of the polymers.

As seen from the fluorescence spectra in Figure 8 and the Stern−Volmer plots in Figure 9, binding of **BU** was associated with a quenching of the fluorescence emission (λ_{em} = 340 nm) of the polymers. This occurred rapidly after addition of the analyte (Figure 10) and contrasts with the recently reported fluorescence enhancement observed for cyclohexylbarbital interacting with an imprinted polymer made using **1**.[23] Possible factors contributing to this conflicting result are the different UV absorptions exhibited by the guests at the excitation wavelength of the fluorophore and the fact that barbiturates are intrinsically fluorescent.

(23) Kubo, H.; Nariai, H.; Takeuchi, T. *Chem. Commun.* **2003**, 2792−2793.

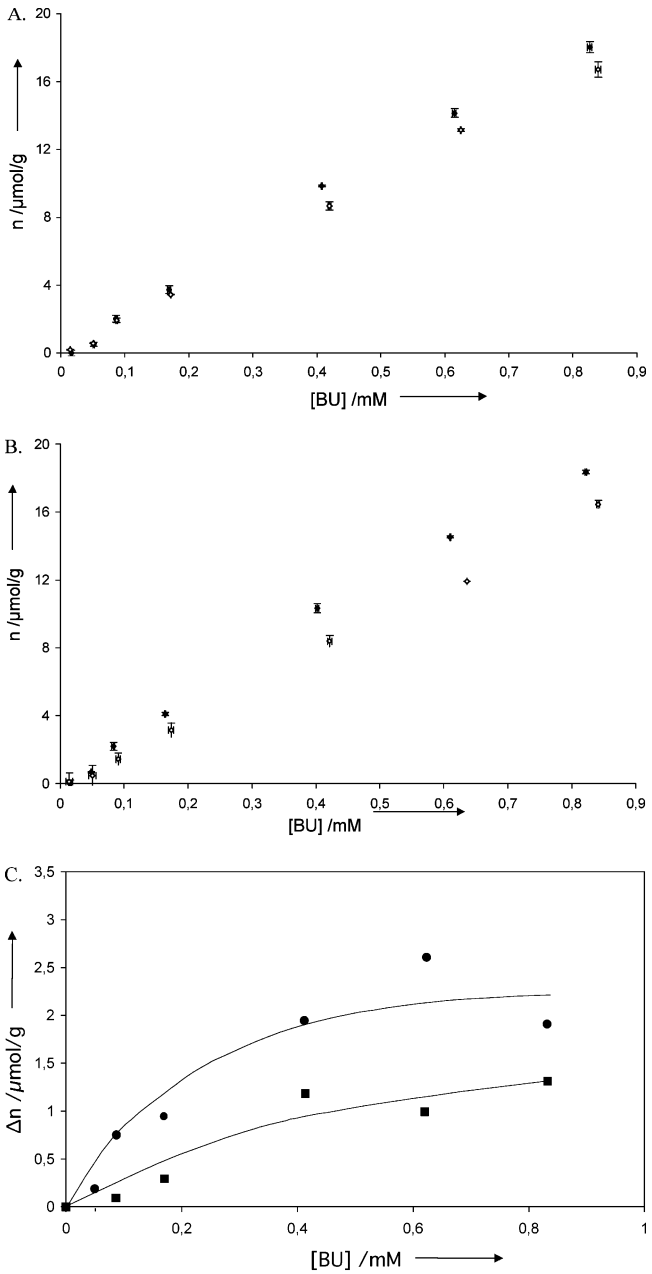

FIGURE 7. Adsorption isotherms in acetonitrile obtained for **BU** adsorbed on (A) **P1** (upper symbols) and $\mathbf{P_N1}$ (lower symbols) and (B) **P2** (upper symbols) and $\mathbf{P_N2}$ (lower symbols) and the corresponding differential plots (C) of **P1** (squares) and **P2** (circles). The data points are the results of two independent experiments where the spread is indicated as error bars. The data have been corrected for bleeding of UV-active material from the polymers.

Also the fluorescence data reveal larger imprinting effects for **P2** than for **P1**, as reflected in the differential plots (Figure 9C). The correlation between the differential Stern−Volmer curves and the corresponding binding isotherms shows that a simple measure of the fluorescence quenching reports on how much template is bound to the polymer.

Why is P2 Better Than P1? To understand the origin of the better performance of the polymers made using **2** we performed a further characterization of the polymers and the solution interactions between **BU** and **2**.

Mode of Monomer Incorporation. Although the elemental analysis data indicated that the monomers had been stoichiometrically incorporated into the polymers the question remained whether they were different concerning the conversion of the second vinyl group. The fluorescence spectral properties of **1** and **2** provided unique structural information concerning the mode of monomer incorporation in the polymer. We found that monomers **1** and **2** exhibited fluorescence emission at 435 nm (on excitation at 270 nm) (Figure 11A) which we anticipated could serve as a direct measure of the accessibility and microenvironment of the imprinted binding sites in the cross-linked polymers.[24]

As seen in Figure 8, the fluorescence spectra corresponding to polymers **P1** and **P2** prepared from monomers **1** and **2**, respectively, displayed emission maxima at ca.340 nm, corresponding to a blue shift of nearly 100 nm compared to the free monomers. Furthermore, the emission intensity was observed to be at least an order of magnitude stronger than for the free monomers. Weaker intensities were also observed at higher wavelengths with a shoulder at 435 nm. It occurred to us that these spectral features could be informative about the mode of monomer incorporation in the polymer. We therefore compared the fluorescence emission spectra (λ_{ex} = 270 nm) of unreacted monomers **1** (Figure 11A) with the model compounds corresponding to monoreacted (**4**) (Figure 11A) and completely reacted (**5**) monomers (Figure 11B). Whereas **1** showed a single broad and weak emission band at 435 nm, the model compound **4** in addition exhibited a weak band at 340 nm. However, model compound **5** showed a single and strong emission peak at 340 nm which coincided with the emission spectra of the polymers. The same result was also obtained when comparing the spectra of **2** and model compound **6**.

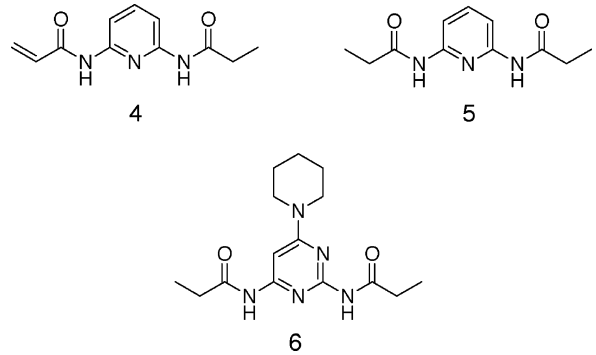

These results suggest that the blue shift is predominantly due to a chemical change in the monomer emission properties upon polymerization rather than microenvironmental effects. Based on these observations we conclude that a significant portion of both monomers (**1** and **2**) has been doubly incorporated in the polymer. The large difference in emission intensity between the model compounds precludes a quantitative evaluation of the data.

Complexation between BU and Monomers Studied by FT-IR. A first inspection of the FT-IR spectra in

(24) Shea, K. J.; Sasaki, D. Y.; Stoddard, G. J. *Macromolecules* **1989**, *21*, 1722.

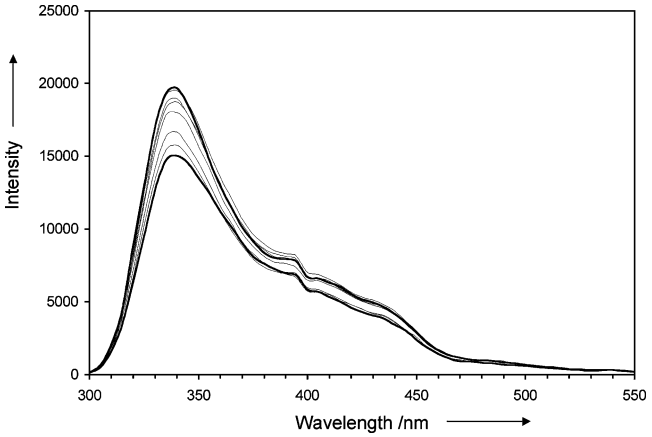

FIGURE 8. Fluorescence emission spectra (λ_{ex} = 270 nm) of **P1** in acetonitrile in the presence of, from top to bottom, increasing amounts of **BU** as described for the experiment in Figure 9.

Figure 6 reveals an interesting and opposite behavior of **1** and **2**. As concluded above, the bands corresponding to neat **1** were broader than those of **2,** indicating the presence of a more defined structure in the latter case. In the presence of a stoichiometric amount of **BU**, the bands of **1** become sharper whereas those of **2** become broader. For **1** the sharpening of the bands is explained by the formation of a well-defined triple hydrogen bonded complex. Further support for this structure is the relatively intense NH bands and the apparent absence of bands corresponding to nonassociated NH. Opposite to the complex between **BU** and **1**, addition of **BU** to **2** appears to result in a less defined structure. This is possibly caused by multiple amide bond conformations or interaction modes *vis-à-vis* **BU**. Studying more closely the high-frequency region, the NH stretch vibrations are found at lower frequencies (even extending below 2800 cm^{-1}) in the complex between **BU** and **2** than those found in neat **2** or in the **BU**-**1** complex. These spectral features indicate the presence of strongly hydrogen-bonded complexes.[22] Another important observation concerns the relative intensities of bands tentatively assigned to *cis*- and *trans*-amide bonds. Addition of **BU** leads to an apparent weakening of the former indicating that the *trans*-conformation is favored. This would be an expected result if **BU** competes for the same interaction sites of **2** as those involved in dimerization.

Complexation between BU and Monomers Studied by ^{1}H NMR. Further attempts to characterize the solution complexes formed between **BU** and **1** and **2**, respectively, were carried out by a closer analysis of the ^{1}H NMR spectra corresponding to the titration of **BU** with **1** or **2**. First it is of interest to identify which of the protons of **BU** experience a complexation induced shift in addition to the imide protons shown in Figure 3 and the extent of these shifts (Table 2). Study of the spectra corresponding to **BU** titrated with **1** revealed downfield shifts of all protons (largest for the pyrimidine ring protons) that saturated at roughly 3 times larger $\Delta\delta_{max}$ than those obtained in the titration with **2**.

Band interference precluded accurate position to be obtained at concentrations of **1** larger than 0.0075 M.

The similar saturation curves and relative $\Delta\delta_{max}$ values indicate that the two monomers interact similarly with

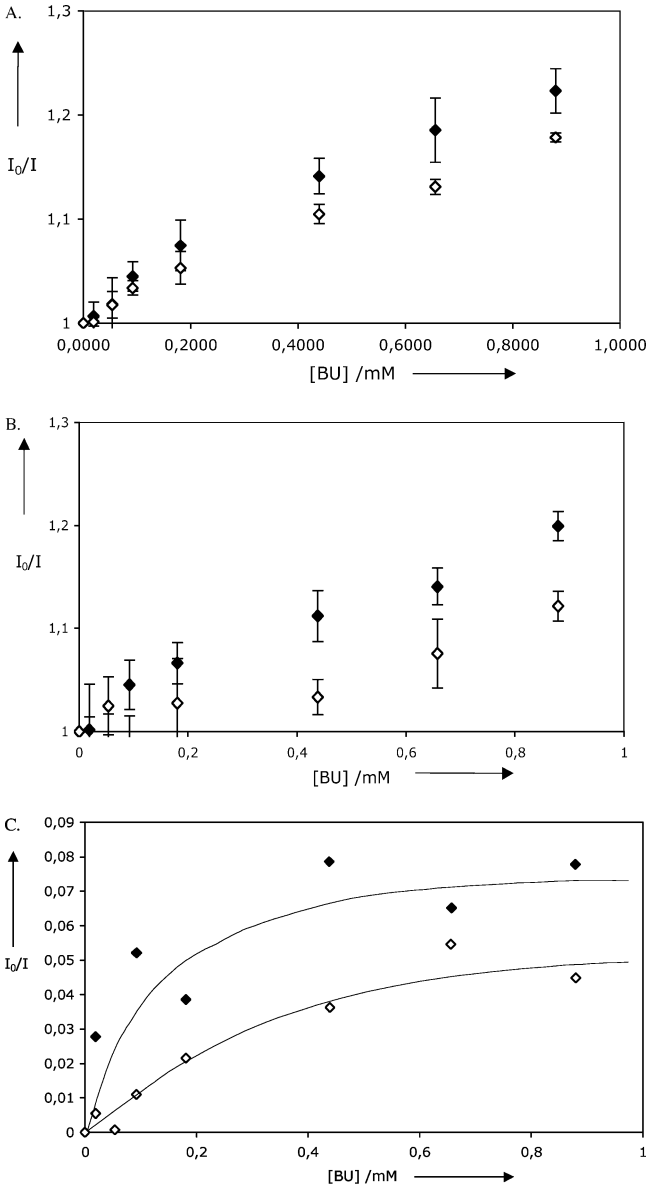

FIGURE 9. Stern−Volmer plots (λ_{ex} = 270 nm, λ_{em} = 340 nm) showing the fluorescence quenching upon addition of **BU** to a suspension of (A) **P1** (solid diamonds) and $\mathbf{P_N1}$ (open diamonds) and (B) **P2** (solid diamonds) and $\mathbf{P_N2}$ (open diamonds) in acetonitrile and the corresponding differential plots (C) of **P1** (open diamonds) and **P2** (solid diamonds). The data points are the average results of independent experiments using two different batches of polymer where the spread is indicated as error bars.

BU. Nevertheless, it does not exclude additional association modes occurring at higher concentrations of **BU** (L) and **2** (S) such as in the prepolymerization mixture (L_t = 20 mM, S_t = 30 mM). The existence of other interaction modes was suggested from a comparison of the spectra of **2** alone with that of an equimolar mixture of **BU** and **2** (Figure 4). Addition of **BU** led to significant downfield shifts of the piperidine i protons whereas the vinyl protons d and f and amide protons a and b shifted upfield (Table 3).

The extent of the shifts of protons d and f were larger but in the same direction as those observed in the dilution experiment of **2**. Of particular interest is the relatively

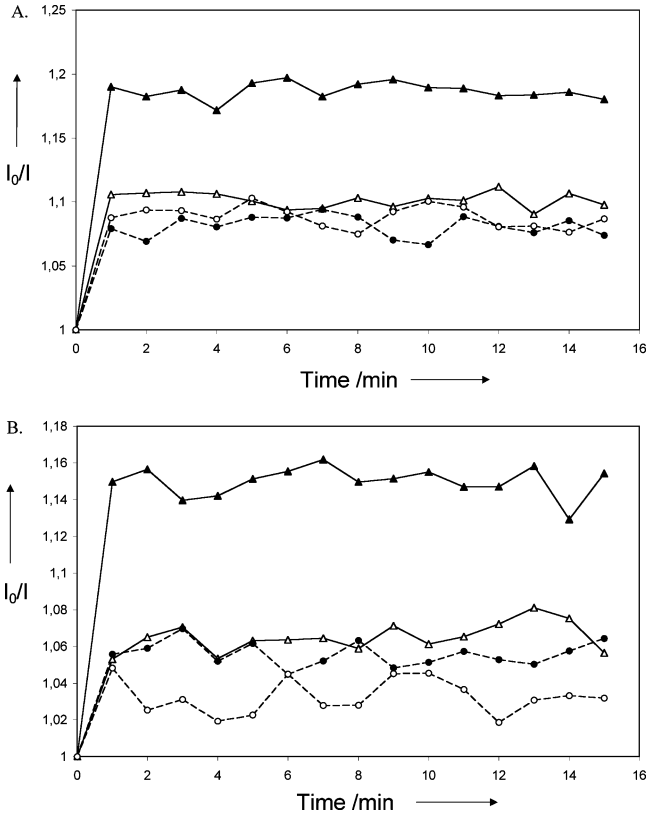

FIGURE 10. Time dependence of the fluorescence quenching (λ_{ex} = 270 nm, λ_{em} = 340 nm) after addition of **BU** (triangles) and **DBU** (circles) to (A) **P1** (solid symbols) and $\mathbf{P_N1}$ (open symbols) and (B) **P2** (solid symbols) and $\mathbf{P_N2}$ (open symbols) in acetonitrile to reach a final concentration of 0.5 mM.

large upfield shift of vinyl proton d. This supports the hypothesis, based on the FT-IR analysis, that **BU** destabilizes the amide *cis*-conformation. The concomitant downfield shift of the piperidine protons i and the appearance of two amide bands indicate that an additional complex species exists at this concentration.

Conclusions

Despite the apparently weaker binding of **BU** displayed by **2** compared to **1**, imprinted polymers made using **2** exhibit increased imprinting effects reflected in higher retention and imprinting factors. We attribute these differences in the properties of the polymers to the binding mode presented by **2** and also its ability to dimerize (Figure 1). Thus, the lower apparent solution binding constant is likely the result of pronounced dimerization of **2** masking the inherently stronger heterocomplex formation **2**:**BU**. These differences are carried through into the polymer matrix during the polymerization step. Template removal exposes the high affinity DAD hydrogen bonding array of **2** whereas the dimers are locked up and are thereby poorly accessible. Possibly, **2** also exposes additional interaction sites for **BU** but the exact nature of these is still unknown. Monomer **1** binds more weakly to **BU** but shows, on the other hand, no tendency to dimerize. The net effect should be the creation of weaker imprinted sites and more pronounced nonspecific binding.

Obviously, molecules incorporating the affinity enhancing features of **2** but unable to dimerize would be of significant interest. In an effort to prevent dimerization we synthesized model compounds **7** and **8** exhibiting more bulky amide substituents which we anticipated

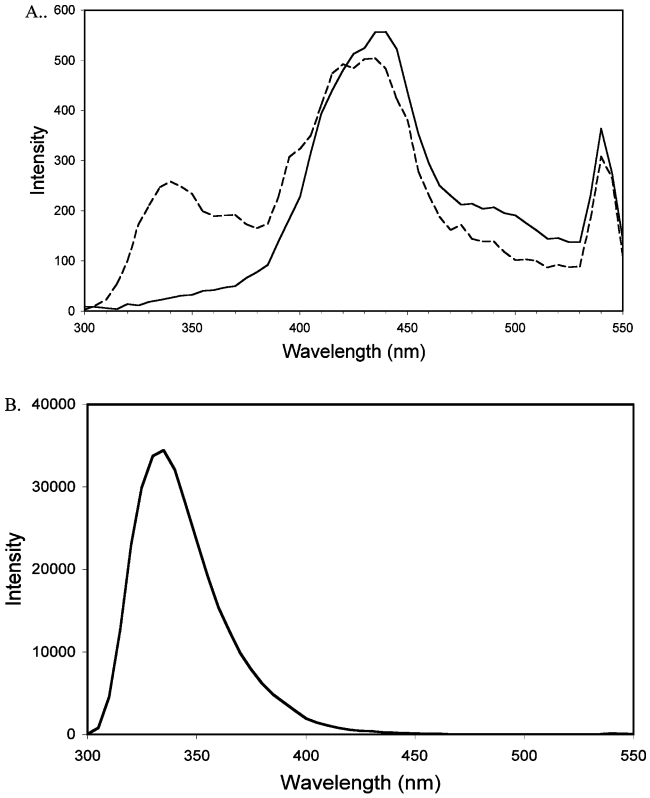

FIGURE 11. Fluorescence emission spectra of (A) model compound **4** (dashed line) and monomer **1** (solid line) and (B) of model compound **5** dissolved in $CHCl_3$ (1 mM). λ_{ex} = 270 nm.

TABLE 2. Complexation-Induced Shifts Observed in the Titration of BU with 1 or 2

		$\Delta\delta_{max}$ (ppm)	
proton	δ start (ppm)	**1**	**2**
Ha′	7.99	+4.19	+1.94
Hb′	5.66	+0.06[a]	+0.04
Hc′	7.13	+0.15	+0.05
Hd′	4.90	+0.08	+0.02
He′,f′,g′	7.34	+0.05	+0.015

[a] Band interference precluded accurate position to be obtained at concentrations of **1** larger than 0.0075 M.

TABLE 3. Complexation-Induced Shifts of 2 Observed in an Equimolar Mixture of BU and 2 (5 mM each in $CDCl_3$) Compared to 2 Alone and upon Dilution of 2 from 10 to 0.8 mM

proton	δ (ppm) 2	$\Delta\delta$ (ppm) **2**+**BU**	$\Delta\delta$ (ppm) **2** dilution
Hj	d 1.578	+0.003	0
Hk	d 1.658	−0.008	−0.01
Hi	s 3.589	+0.023	0
Hf,g	m 5.745	−0.016	+0.02
He,h	m 6.438	+0.002	0
Hc	q 6.660	−0.035	−0.12
Hd	q 7.228	−0.18[a]	−0.05
Hl	s 7.444	−0.005	−0.01
Ha,b	s 10.93	−0.25[b]	−1.0

[a] Broadened quartet. [b] Signal appeared as two peaks at 10.65 and 10.72 ppm.

would stabilize the amide trans isomer and thus prevent dimerization.[27]

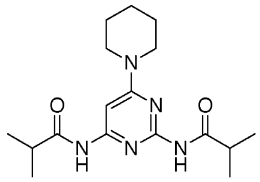

7

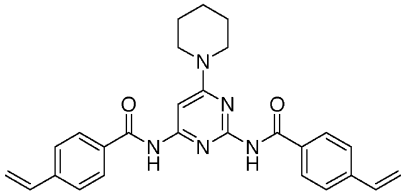

8

Whereas **7** exhibited similar dimerization behavior as **2** judged from IR and NMR data, **8** alone showed IR spectra more similar to **1**. However, addition of BU to **8** did not lead to disappearance of the bands corresponding to free NH groups (see Supporting Information) indicating that these interacted weakly compared to **1** and **2**. This was further supported by the low chromatographic imprinting factors obtained for polymers prepared against **BU** using **8** as functional monomer.

An interesting property of the system is the correlation between the ligand binding with the extent of fluorescence quenching. Although fluorescence reporter groups have been incorporated in imprinted binding sites previously,[25,26] the use of simple DAD monomers as combined binding and reporter groups has only recently been reported.[23] The enhanced affinity *vis-à-vis* imides using **2**, seems promising for the future design of polymers for the separation and sensing of such guests.

Acknowledgment. Work supported in part by the European Community's Training and Mobility Program under Contract No. FMRX-CT-98-0173 [MICA] and by Heineken Technical Services (Zoeterwoude, NL).

Supporting Information Available: FTIR spectra and chromatographic retention data. This material is available free of charge via the Internet at http://pubs.acs.org.

JO0477906

(25) Turkewitsch, P.; Wandelt, B.; Darling, G. D.; Powell, W. S. *Anal. Chem.* **1998**, *70*, 2025−2030.

(26) Matsui, J.; Higashi, M.; Takeuchi, T. *J. Am. Chem. Soc.* **2000**, *122*, 5218−5219.

(27) Early attempts to synthesise the methacrylamide version of **2** failed due to its unexpectedly high tendency to polymerize. This may in itself be an indication that also this molecule prefers the cis isomer resulting in a less conjugated double bond.